

AGN FEEDBACK CAUSES DOWNSIZING

EVAN SCANNAPIECO,¹ JOSEPH SILK,² AND RYCHARD BOUWENS³

Received 2005 August 17; accepted 2005 November 1; published 2005 November 23

ABSTRACT

We study the impact of outflows driven by active galactic nuclei (AGNs) on galaxy formation. Outflows move into the surrounding intergalactic medium (IGM) and heat it sufficiently to prevent it from condensing onto galaxies. In the dense, high-redshift IGM, such feedback requires a highly energetic outflow, driven by a large AGN. However, in the more tenuous low-redshift IGM, equivalently strong feedback can be achieved by less energetic winds (and thus smaller galaxies). Using a simple analytic model, we show that this leads to the *antihierarchical* quenching of star formation in large galaxies, consistent with current observations. At redshifts prior to the formation of large AGNs, galaxy formation is hierarchical and follows the growth of dark matter halos. The transition between the two regimes lies at the $z \approx 2$ peak of AGN activity.

Subject headings: galaxies: evolution — large-scale structure of universe — quasars: general

Online material: color figure

1. INTRODUCTION

Downsizing is not a recent trend. For the past 10 billion years, the characteristic stellar mass of forming galaxies has been decreasing, as demonstrated by a variety of observations. Space-based near-ultraviolet measurements show that the typical star formation rate (SFR) in galaxies was over an order of magnitude higher at $z = 3$ than at $z = 0$ (Arnouts et al. 2005). Ground-based optical and near-infrared searches indicate that the largest galaxies were already in place by $z \approx 2$, while smaller ones continued to form stars at much lower redshifts (Fontana et al. 2004; Glazebrook et al. 2004; van Dokkum et al. 2004; Treu et al. 2005). And both optical and X-ray surveys detect a steady decrease in the characteristic luminosity of active galactic nuclei (AGNs) below $z \approx 3$ (Pei 1995; Ueda et al. 2003), which is likely to parallel the formation history of early-type galaxies (e.g., Granato et al. 2001, 2004).

Yet despite such widespread evidence, galaxy downsizing (Cowie et al. 1996) was unexpected. The Λ cold dark matter (Λ CDM) model, while in spectacular agreement with observations (e.g., Spergel et al. 2003), is a hierarchical theory, in which gravitationally bound subunits merge and accrete mass to form ever-larger objects. Superposed on this DM distribution is the observed baryonic component. In canonical models, this gas falls into potential wells, is shocked-heated to the virial temperature, and must radiate this energy away before forming stars (Rees & Ostriker 1977; Silk 1977). The larger the structure, the higher its virial temperature, and the longer it takes to cool. Also, in most semianalytical models, the dynamical timescale is adopted for the rate of star formation via the Schmidt-Kennicutt law, and this timescale increases systematically with halo mass. Thus, larger galaxies were expected to form later not only because they occur in later forming dark matter halos but because the cooling and star formation times within such halos are longer.

Two recent lines of inquiry have modified this picture. Theoretically, simulations have shown that cooling is greatly en-

hanced by gas inhomogeneities, allowing galaxies to form with stellar masses over 10 times larger than observed (Suginohara & Ostriker 1998; Davé et al. 2001). In fact, virializing shocks may even be completely absent in smaller halos (Birnboim & Dekel 2003). Observationally, it has been discovered that the main heating source for groups and small galaxy clusters is nongravitational (e.g., Arnaud & Evrard 1999). As these are the gaseous halos that were slightly too massive to form into galaxies, the clear implication is that nongravitational heating also played a key role in the history of large galaxies.

Furthermore, the ≈ 1 keV per gas particle necessary to preheat the intracluster medium (ICM) appears to exceed the energy available from supernovae (e.g., Valageas & Silk 1999; Wu et al. 2000; Kravtsov & Yepes 2000). At the same time, AGNs are observed to host high-velocity outflows with kinetic luminosities that may equal a significant fraction of their bolometric luminosity (e.g., Chartas et al. 2002; Pounds et al. 2003; Morganti et al. 2005; see, however, Sun et al. 2005). Such outflows would naturally preheat the ICM to the necessary levels (Roychowdhury et al. 2004; Lapi et al. 2005), placing this gas at an entropy at which it cannot cool within a Hubble time (Voit & Brian 2001; Oh & Benson 2003). This results in a feedback-regulated picture of galaxy formation fundamentally different from the canonical approach (Scannapieco & Oh 2004; Binney 2004; Di Matteo et al. 2005).

In this Letter, we explore the connection between this developing picture and the widespread observations of downsizing, structuring our investigation as follows: In § 2 we develop a simple cooling model for galaxy formation, which illustrates how hierarchical formation naturally arises in the canonical approach. In § 3 we modify our model to include AGN feedback, and show how this leads to a radically different, antihierarchical history. We compare these results with recent observations and conclude with a short discussion in § 4.

2. A COOLING-REGULATED MODEL OF GALAXY FORMATION

Throughout this study, we assume a Λ CDM model with parameters $h = 0.65$, $\Omega_0 = 0.3$, $\Omega_\Lambda = 0.7$, $\Omega_b = 0.05$, $\sigma_8 = 0.87$, and $n = 1$, where h is the Hubble constant in units of $100 \text{ km s}^{-1} \text{ Mpc}^{-1}$, Ω_0 , Ω_Λ , and Ω_b are the total matter, vacuum energy, and baryonic densities in units of the critical density, σ_8^2 is the variance of linear fluctuations on the $8 h^{-1} \text{ Mpc}$ scale, and n is

¹ Kavli Institute for Theoretical Physics, University of California at Santa Barbara, Kohn Hall, Santa Barbara, CA 93106-4030.

² Astrophysics Department, University of Oxford, Keble Road, Oxford OX1 3RH, UK.

³ Astronomy Department, University of California at Santa Cruz, 477 Clark Kerr Hall, Santa Cruz, CA 95064.

the “tilt” of the primordial power spectrum (e.g., Spergel et al. 2003). The Eisenstein & Hu (1999) transfer function is adopted.

We begin with a model of cooling-regulated galaxy formation and adopt as simple an approach as possible, to highlight the key physical issues. Unlike more sophisticated approaches (e.g., Kauffmann et al. 1993; Somerville & Primack 1999; Benson et al. 2000), we do not attempt to trace the detailed history of a sample of DM halos through the use of statistical “merger trees.” Instead, we use the fit described in van den Bosch (2002), which gives the *average* history of a DM halo with a present total mass of M_0 as

$$\log \left[\frac{M(z)}{M_0} \right] = -0.301 \left[\frac{\log(1+z)}{\log(1+z_{\text{fit}})} \right]^\nu, \quad (1)$$

where $\nu \equiv 1.34 + 1.86 \log(1+z_{\text{fit}}) - 0.03 \log(M_0/10^{12} M_\odot)$, $M(z)$ is the mass of this system at some redshift z , and z_{fit} is defined implicitly through the relation $D(z_{\text{fit}})^{-1} = 1 + 0.40[\sigma^2(0.254M_0) - \sigma^2(M_0)]^{1/2}$, with D being the linear growth factor and $\sigma^2(M_0)$ being the variance of linear fluctuations within a sphere enclosing a total mass M .

Following the canonical picture, we assume that at each redshift, gas flows onto the growing halo along with the dark matter, is shocked to its virial density and temperature at that redshift (180 times the mean density and $7.2 \times 10^5 [M(z)/10^{12} M_\odot]^{2/3} (1+z)$ K, respectively), and is finally added to the pool of cold gas that forms stars after a delay of

$$t_{\text{cool}} = 1.3 T_6 \langle n_e \rangle^{-1} C^{-1} \Lambda_{-23}^{-1} (T_6) \text{ Myr}. \quad (2)$$

Here $\langle n_e \rangle$ is the average number of electrons per cm^3 in the shocked gas, $C \equiv \langle n_e^2 \rangle \langle n_e \rangle^{-2}$ is a “clumping factor,” which accounts for inhomogeneities, T_6 is the temperature in units of 10^6 K, and Λ_{-23} is the radiative cooling rate of the gas in units of $10^{-23} \text{ ergs cm}^3 \text{ s}^{-1}$. Near 1 keV $\approx 10^7$ K, Λ_{-23} is roughly a constant, but, in general, it is a function of temperature and metallicity. For simplicity, we adopt the Sutherland & Dopita (1993) equilibrium values for this rate at a fixed metallicity of $0.1 Z_\odot$, the level of pre-enrichment of G dwarf stars in the solar neighborhood (Ostriker & Thuan 1975) and in large neighboring galaxies (Thomas et al. 1999). Finally, in keeping with previous semianalytical models, we ignore gas inhomogeneities, taking $C = 1$. Adopting a larger value, consistent with simulations, would result in the same overall trends, but with galaxies that were much too large.

We then compute the mass of cooled gas as a function of the total mass and redshift of the observation, as illustrated in Figure 1. Here we see the classic behavior first described in Rees & Ostriker (1977) and Silk (1977). As their cooling times are short, $M_{\text{cool}}/M_{\text{tot}} \approx \Omega_b/\Omega_0$ in small objects, while for larger masses with longer cooling times, $M_{\text{cool}}/M_{\text{tot}} \ll \Omega_b/\Omega_0$. In this picture, the maximum $M_{\text{cool}}(z)$ is the largest gas mass that has time to virialize and cool, a value that increases with time. Roughly, one can estimate this scaling as $t_{\text{cool},i} = t_f \propto (1+z_f)^{-3/2}$, where t_f and z_f are the final time and redshift at which the gas cools, respectively, while $t_{\text{cool},i}$ is computed at the initial redshift at which the gas falls on the halo. For the accretion histories described by equation (1), T_{vir} depends only weakly on redshift, which allows us to rewrite this as $M_{\text{cool}} \propto (1+z_f)^{-3/4} T_{\text{vir}}$.

In Figure 1 we also compute the average redshift of for-

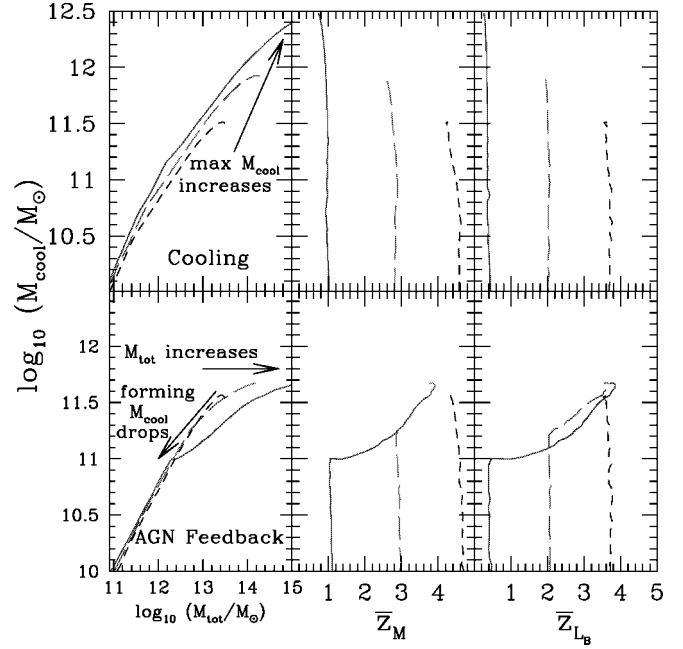


FIG. 1.—Mass of cooled gas in models regulated by cooling (*top panels*) and AGN feedback (*bottom panels*). In both cases, the left panels compare the cooled gas mass with the total mass, the middle panels give the mass-averaged star formation redshift, and the right panels give the luminosity-weighted (*B*-band) average star formation redshift. In all panels, the solid, long-dashed, and short-dashed lines correspond to galaxies observed at redshifts of 0, 1.5, and 3 respectively. In the cooling-regulated models (§ 2), larger galaxies continue to form at late times, and all galaxies are dominated by young stars. In the models regulated by AGN feedback (§ 3), the maximum scale of forming galaxies decreases with time, and large galaxies are accreted into bigger halos without forming new stars. When observed at low redshift, the stars in these objects are older. [See the electronic edition of the *Journal* for a color version of this figure.]

mation of the resulting stars, adopting both a mass average, that is, $\bar{z}_M = z(\bar{t}_M)$, where

$$\bar{t}_M \equiv \frac{\int_0^{t_{\text{obs}}} dt' t' \dot{M}_{\text{cool}}}{\int_0^{t_{\text{obs}}} dt' \dot{M}_{\text{cool}}}, \quad (3)$$

and a *B*-band luminosity-weighted average, that is, $\bar{z}_{LB} = z(\bar{t}_{LB})$, where

$$\bar{t}_{LB} \equiv \frac{\int_0^{t_{\text{obs}}} dt' t' \dot{M}_{\text{cool}} \Upsilon_B^{-1}(t_{\text{obs}} - t')}{\int_0^{t_{\text{obs}}} dt' \dot{M}_{\text{cool}} \Upsilon_B^{-1}(t_{\text{obs}} - t')}; \quad (4)$$

here $\Upsilon_B(t)$ is the *B*-band mass-to-light ratio of a population of stars with an age t , assuming a Salpeter initial mass function as computed by Bruzual & Charlot (2003). In all cases, \bar{z}_M and \bar{z}_{LB} are very close to the observed redshifts, meaning that in objects of all masses and redshifts, most of the stellar mass and luminosity comes from recently formed stars.

3. A FEEDBACK-REGULATED MODEL OF GALAXY FORMATION

We now modify our model to include AGN feedback, adopting an approach that parallels Scannapieco & Oh (2004), itself an extension of Wyithe & Loeb (2003). These papers showed that imposing an $M_{\text{BH}} \propto v_c^5$ relationship between black hole mass and halo circular velocity (Ferrarese 2002) and assuming that these objects shine at their Eddington luminosity for a fraction of the dynamical time after each major merger give a good fit to the

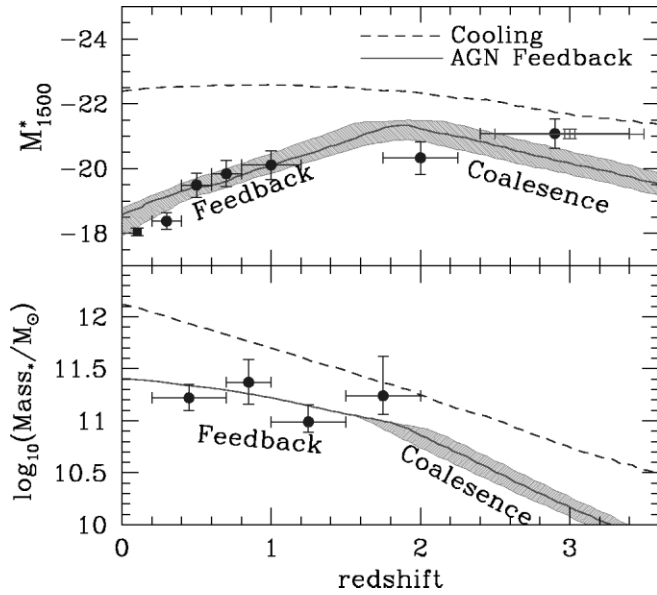


FIG. 2.—*Top*: Evolution of M_{1500}^* , the characteristic scale for the instantaneous SFR in galaxies. The lines are from our cooling model (dashed) and $\epsilon_k = 0.05$ AGN feedback model (solid), compared with measurements by Arnouts et al. (2005; filled circles) and Steidel et al. (1999; open square). *Bottom*: Evolution of the characteristic stellar mass as compared to measurements by Fontana et al. (2004). The lines are the same as in the upper panel. In both panels, the shaded regions correspond to AGN feedback models with ϵ_k varied from 0.025 to 0.1. The AGN feedback model is divided into two regimes: a high-redshift (“coalescence”) regime, in which the characteristic scale of star-forming galaxies increases with the nonlinear mass scale, and a low-redshift (“feedback”) regime, in which this characteristic scale decreases as a result of quenching from ever more efficient feedback. [See the electronic edition of the Journal for a color version of this figure.]

observed AGN luminosity function. In particular, each merger with a mass ratio less than 4 : 1 was associated with an AGN with a total bolometric energy (in units of 10^{60} ergs) of

$$E_{60, \text{bol}} = 23M_{12, \text{cool}}^{5/3}(1+z), \quad (5)$$

where $M_{12, \text{cool}}$ is the mass of cooled gas in units of $10^{12} M_\odot$.

Each AGN was then taken to host an outflow, with a total kinetic energy equal to $\epsilon_k \approx 0.05$ of the total bolometric energy. Adopting a Sedov-Taylor model, this resulted in a postshock temperature of $T_s(R) = 8.8 \times 10^6 \epsilon_k E_{60, \text{bol}} M_{12, \text{gas}}^{-1}(R)$, where $M_{12, \text{gas}}$ is the total gas mass contained with a radius R in units of $10^{12} M_\odot$. Our simple model here does not distinguish between merger events, and so instead we relate the *change* in temperature at a radius R to the *change* in cooled mass by replacing $M_{12, \text{cool}}$ with $dM_{12, \text{cool}}$:

$$\frac{dT_s(R)}{dM_{12, \text{cool}}} = 2.0 \times 10^8 \epsilon_k \frac{M_{12, \text{cool}}^{2/3}(1+z)}{M_{12, \text{gas}}(R)} \text{ K}. \quad (6)$$

Apart from this additional contribution to the temperature, our model exactly parallels that in § 2, with two minor modifications. First, if a parcel of gas remains at a temperature above the final virial temperature of the halo for a time longer than its dynamical time, we assume it escapes from the gravitational potential. Second, we choose the clumping factor to be consistent with simulations, which show that roughly 40% of the gas cools onto galaxies by $z = 0$ in the absence of feedback (Davé et al. 2001; Balogh et al. 2001). This requires

us to raise M_{cool} (without feedback) by a factor of ~ 30 , which corresponds to $C \approx 3$.

With these modifications, and adopting a fiducial value of $\epsilon_k = 0.05$, we constructed plots of M_{cool} , \bar{z}_M , and \bar{z}_{L_B} as in § 2. These are shown in the lower panels of Figure 1. As in our cooling model, $M_{\text{cool}}/M_{\text{tot}} \approx \Omega_b/\Omega_0$, in small halos, where feedback is weak. At large masses, however, feedback causes M_{cool} to evolve radically differently. Now the maximum scale of star-forming galaxies *drops* at lower redshifts. This is the direct result of the decrease in the cosmological gas density and the fact that at lower redshifts, smaller AGNs (and hence smaller galaxies) can heat this gas to temperatures that will not cool within a dynamical time. The scaling of this “quenching threshold” (Faber et al. 2005) can be estimated by setting the dynamical time ($\propto n^{-1/2}$) equal to the post-AGN feedback cooling time given by equations (2) and (5). For the ≈ 1 keV objects we are interested in, this gives $M_{\text{cool}} \propto (1+z)^{3/4}$.

Galaxies with the largest M_{cool} values ($\approx 3 \times 10^{11} M_\odot$) are already in place at $z = 3$ and continue to fall into larger halos at lower z without increasing in stellar mass. Somewhat smaller $M_{\text{cool}} \approx 10^{11} M_\odot$ galaxies can recover from an AGN outflow at $z = 1.5$, but not at the lowest redshifts. Finally, galaxies with $M_{\text{cool}} < 10^{11} M_\odot$ can hold onto their gas, even at $z = 0$. Note, however, that our simple models do not include supernova feedback, which is likely to be important in galaxies with $M_{\text{tot}} \lesssim 10^{11} M_\odot$ (Martin 1999). This mechanism should behave qualitatively differently, as it depends primarily on momentum transfer rather than heating (Thacker et al. 2002). Note also that we do not account for the possibility of initial positive AGN feedback before quenching occurs, as may be required by observations of efficient star formation in massive high-redshift galaxies (Silk 2005).

The antihierarchical trend in our model is also apparent from the mass and B -band luminosity-weighted ages. In small galaxies, most of the stars are relatively young and were formed at redshifts close to the redshifts of observation. Stars in large galaxies, however, are much older, and their ages increase as a function of M_{cool} .

4. COMPARISON WITH OBSERVATIONS AND DISCUSSION

The features of the simple models developed in §§ 2 and 3 can be directly compared with observations. As a measure of the typical SFR, we compute the absolute AB magnitude at 1500 Å for our model galaxies, assuming that 50% of the cooled gas is in the form of stars, adopting the Bruzual & Charlot (2003) population synthesis models, and ignoring dust. We do not attempt to construct a luminosity function of galaxies, since doing so would require us to use a full merger-tree formalism. Rather, for both cooling and AGN feedback models, we impose a halo mass limit of $\nu(M_{\text{NL}}, z) = \delta_c \sigma(M)^{-1} D(z)^{-1} \leq 2.5$ at each redshift, to exclude excessively rare peaks. For the CDM power spectrum at these redshifts, $M_{\text{NL}} \propto (1+z)^{-6}$, such that the corresponding virial temperature $T_{\text{vir, NL}} \propto (1+z)^{-3} \propto M_{\text{NL}}^{1/2}$.

We then find the most luminous galaxy at 1500 Å within the remaining halos and plot its absolute magnitude as a function of redshift in the upper panel of Figure 2. This is compared with the observed evolution of M_{1500}^* to $z \sim 3$, which is divided into two regions. At high redshift, it brightens along with the nonlinear mass scale over the dynamical time. At low redshift, the most luminous galaxies no longer lie in the largest halos. Rather, M_{1500}^* fades along with the AGN quenching mass scale over t_{dyn} . The redshift at which these two scales cross marks a distinct transition between hierarchical and antihierarchical

TABLE 1
PROPERTIES OF GALAXY FORMATION MODELS

Model	Characteristic M_{cool} at High z	Characteristic M_{cool} at Low z	Characteristic SFR at Low z	$z = 0$ Trends
Cooling	Tracks M_{NL} , (1 + z) ⁻⁶	Cooling-regulated, (1 + z) ^{-3/2}	$M_{\text{cool}}/t_{\text{dyn}}$ roughly constant	Bigger galaxies are young and blue
AGN feedback	Tracks M_{NL} , (1 + z) ⁻⁶	Feedback-regulated, (1 + z) ^{3/4}	$M_{\text{cool}}/t_{\text{dyn}}$, (1 + z) ^{3/4}	Bigger galaxies are older and redder

NOTE.—Scaling relationships are approximate.

growth, which occurs at the peak of AGN activity (e.g., Pei 1995; Ueda et al. 2003).

The shaded regions in this figure show the impact of varying ϵ_k , which shifts the peak value of M_{1500}^* . Modifying our other assumptions (M_{NL} , cold fraction in stars, etc.) would result in similar changes. In particular, dust would cause M_{1500}^* to saturate at $z \approx 2$ due to the larger attenuation factors of large starbursts (e.g., Wang & Heckman 1996; Adelberger & Steidel 2000; Martin et al. 2005). Our point is not to fit these particular parameters to the data, however, but rather that substantial high-redshift brightening and lower redshift fading of M_{1500}^* are general and unavoidable features of AGN-regulated galaxy formation.

Coincidentally, this sharp peak in M_{1500}^* is now starting to be seen observationally. Whereas it has been known for several years that M^* brightens monotonically from $z \approx 0$ to $z \approx 2$ in the UV and bluer optical bands (e.g., Gabasch et al. 2004; Arnouts et al. 2005), recent measurements at $z \approx 5$ –6 (Ouchi et al. 2004; Bouwens et al. 2005) now also show a downturn relative to lower redshifts, implying that M_{1500}^* is most luminous around $z \approx 3$. Remarkably, this is very close to the peak in AGN activity, suggesting that $z \approx 2$ –4 represents the key epoch for gas accretion onto massive systems.

Turning our attention to the evolution of the maximum stellar mass, as shown in the bottom panel of Figure 2, similar trends are apparent. While the maximum mass in the cooling model

increases monotonically, the AGN feedback model is divided into two regions: one at high redshift, in which the maximum stellar mass increases along with the nonlinear mass scale, and one at low redshift, in which the maximum stellar mass stays fixed as the scale at which new galaxies are forming becomes smaller. The general properties of cooling and AGN feedback models are summarized in Table 1.

Finally, we point out that not only is the temporal distribution of AGNs in our feedback model suggestive of recent observations but so is the *spatial* distribution. Using over 20,000 galaxies from the 2dF QSO Redshift Survey, Croom et al. (2005) have studied the spatial clustering of QSOs near the characteristic scale in the optical luminosity function. They measure bias values that, when converted into $\nu(z)$ values using standard expressions (Mo & White 1996), evolve from 2.5 ± 0.2 at $z = 2.48$ down to 1.1 ± 0.2 at $z = 0.56$. The characteristic scale of low-redshift AGNs is downsizing from the rarest to the most common objects, spreading the heated gas that extinguishes the formation of galaxies to this day.

We thank Biman Nath, Chris Reynolds, and Tomasso Treu for helpful comments. This work was initiated during a visit by J. S. to the KITP as part of the Galaxy-IGM Interactions Program. E. S. was supported by the NSF under grant PHY99-07949.

REFERENCES

- Adelberger, K. L., & Steidel, C. C. 2000, *ApJ*, 544, 218
 Arnaud, A., & Evrard, A. E. 1999, *MNRAS*, 305, 631
 Arnouts, S., et al. 2005, *ApJ*, 619, L43
 Balogh, M. L., Pearce, F. R., Bower, R. G., & Kay, S. T. 2001, *MNRAS*, 326, 1228
 Benson, A. J., Cole, S., Frenk, C. S., Baugh, C. M., & Lacey, C. G. 2000, *MNRAS*, 311, 793
 Binney, J. 2004, *MNRAS*, 347, 1093
 Birnboim, Y., & Dekel, A. 2003, *MNRAS*, 345, 349
 Bouwens, R. J., Illingworth, G. D., Blakeslee, J. P., & Franx, M. 2005, *ApJ*, in press (astro-ph/0509641)
 Bruzual, G., & Charlot, S. 2003, *MNRAS*, 344, 1000
 Chartas, G., Brandt, W. N., Gallagher, S. C., & Garmire, G. P. 2002, *ApJ*, 579, 169
 Cowie, L. L., Songaila, A., Hu, E. M., & Cohen, J. G. 1996, *AJ*, 112, 839
 Croom, S. M., et al. 2005, *MNRAS*, 356, 415
 Davé, R., et al. 2001, *ApJ*, 552, 473
 Di Matteo, T., Springel, V., & Hernquist, L. 2005, *Nature*, 433, 604
 Eisenstein, D. J., & Hu, W. 1999, *ApJ*, 511, 5
 Faber, S. M., et al. 2005, *ApJ*, submitted (astro-ph/0506044)
 Ferrarese, L. 2002, *ApJ*, 578, 90
 Fontana, A., et al. 2004, *A&A*, 424, 23
 Gabasch, A., et al. 2004, *A&A*, 421, 41
 Glazebrook, K., et al. 2004, *Nature*, 430, 181
 Granato, G. L., et al. 2001, *MNRAS*, 324, 757
 ———. 2004, *ApJ*, 600, 580
 Kauffmann, G., White, S. D. M., & Guiderdoni, B. 1993, *MNRAS*, 264, 201
 Kravtsov, A. V., & Yepes, G. 2000, *MNRAS*, 318, 227
 Lapi, A., Cavaliere, A., & Menci, N. 2005, *ApJ*, 619, 60
 Martin, C. L. 1999, *ApJ*, 513, 156
 Martin, D. C., et al. 2005, *ApJ*, 619, L1
 Mo, H. J., & White, S. D. M. 1996, *MNRAS*, 282, 347
 Morganti, R., Tadhunter, C. N., & Oosterloo, T. A. 2005, *A&A*, in press (astro-ph/0510263)
 Oh, S. P., & Benson, A. 2003, *MNRAS*, 342, 664
 Ostriker, J. P., & Thuan, T. X. 1975, *ApJ*, 202, 353
 Ouchi, M., et al. 2004, *ApJ*, 611, 660
 Pei, Y. C. 1995, *ApJ*, 438, 623
 Pounds, K., King, A. R., Page, K. L., & O'Brien, P. T. 2003, *MNRAS*, 346, 1025
 Rees, M. J., & Ostriker, J. P. 1977, *MNRAS*, 179, 541
 Roychowdhury, S., Ruszkowski, M., Nath, B. B., & Begelman, M. C. 2004, *ApJ*, 615, 681
 Scannapieco, E., & Oh, S. P. 2004, *ApJ*, 608, 62
 Silk, J. 1977, *ApJ*, 211, 638
 ———. 2005, *MNRAS*, in press (astro-ph/0509149)
 Somerville, R. S., & Primack, J. R. 1999, *MNRAS*, 310, 1087
 Spergel, D. N., et al. 2003, *ApJS*, 148, 175
 Steidel, C. C., Adelberger, K. L., Giavalisco, M., Dickinson, M., & Pettini, M. 1999, *ApJ*, 519, 1
 Sugimoto, T., & Ostriker, J. P. 1998, *ApJ*, 507, 16
 Sun, M., Jerius, D., & Jones, C. 2005, *ApJ*, 633, 165
 Sutherland, R. S., & Dopita, M. A. 1993, *ApJS*, 88, 253
 Thacker, R. J., Scannapieco, E., & Davis, M. 2002, *ApJ*, 581, 836
 Thomas, D., Greggio, L., & Bender, R. 1999, *MNRAS*, 302, 537
 Treu, T., Ellis, R. S., Liao, T. X., & van Dokkum, P. G. 2005, *ApJ*, 622, L5
 Ueda, Y., Akiyama, M., Ohta, K., & Miyaji, T. 2003, *ApJ*, 598, 886
 Valageas, P., & Silk, J. 1999, *A&A*, 350, 725
 van den Bosch, F. C. 2002, *MNRAS*, 331, 98
 van Dokkum, P. G., et al. 2004, *ApJ*, 611, 703
 Voit, M., & Brian, G. 2001, 2001, *Nature*, 414, 425
 Wang, B., & Heckman, T. M. 1996, *ApJ*, 457, 645
 Wu, K. K. S., Fabian, A., & Nulsen, P. E. J. 2000, *MNRAS*, 318, 889
 Wyithe, J. S. B., & Loeb, A. 2003, *ApJ*, 595, 614